JOURNAL OF MATERIALS SCIENCE 27 (1992) 2914–2921

Phosphate glass–ceramic–cobalt–chromium composite materials

F. PERNOT, R. ROGIER*
*Laboratoire de Science des Matériaux Vitreux, CNRS, URA 1119,
USTL Place E. Bataillon, 34095 Montpellier Cédex 05, France*

Phosphate glass–ceramic–cobalt–chromium particulate composites have been prepared by hot-pressing and their thermal, elastic and mechanical properties have been measured. Results have then been explained using various theoretical models on thermal properties, elasticity and fracture mechanics of particulate composites. It is shown that the evolution of average thermal expansion coefficients as a function of cobalt–chromium volume fraction agrees well with Turner's model [25]. In the same way, Young's moduli lie within Hashin and Shtrickman's upper and lower bounds [33], which means both a close contact between matrix and particles and no microcracking of materials. Strength and fracture toughness do not show significant evolutions with metal volume fraction. Fracture energy continuously decreases which produces both a nearly planar surface fracture and a poor bonding between matrix and particles.

1. Introduction

Composite materials have been a subject of intensive interest during the last four decades. Such materials have been developed to achieve a combination of properties not achievable by any of the elemental materials acting alone. Many potential applications exist for these materials [1].

In the field of biomedical materials, calcium alumino-phosphate glass–ceramic–metal particulate composites have been prepared previously. They have been proposed to carry out thermal and elastic graded seals between various dense metal cores of prostheses and a porous phosphate glass–ceramic coating [2, 3].

Their method of synthesis has been investigated. Their thermal and elastic properties have been measured mainly to determine that they lie within the parameters of the phosphate glass–ceramic matrix and of the corresponding metallic reinforcement (titanium, 316 L stainless steel, cobalt chromium 788 alloy) [2, 4].

Detailed studies on thermal, elastic behaviour and fracture mechanics of phosphate glass–ceramic–titanium composites have also been performed [5]. However, these parameters have not yet been investigated thoroughly for other phosphate glass–ceramic–metal composites previously proposed for orthopaedic applications. This paper deals with basic understanding on thermal and deformation behaviour, strength and toughness of phosphate glass–ceramic–cobalt–chromium particulate composites.

2. Experimental procedure

2.1. The base products and preparation of composites

The parent calcium alumino phosphate glass "CAP" is composed of 69.0% P_2O_5, 22.7% CaO, 8.3% Al_2O_3 in weight ratio. It is prepared by mixing suitable proportions of calcium bis-dihydrogen phosphate and hydrated aluminium orthophosphate and melting the mixture in a Pt–10% Rh crucible at 1300 °C for 2 h. The glass is then milled to a particle size of less than 50 μm.

Cobalt–chromium alloy (788 Metafram), has the following compositional brackets for the more important alloying elements: 25–29% Cr, 5–6% Mo, 1.75–3.75% Ni, 0.8–2% Si, 0.2–0.3% C, balance cobalt, in weight ratio. Spheres are purchased in bulk form, then separated into three size fractions (average particle diameters 22, 40 and 60 μm) by sieves. A fraction of the smallest sized particles (22 μm) is oxidized in air atmosphere at 800 °C for various times (1–100 h). The oxidation treatments are evaluated by weight gain tests (Fig. 1).

Properties of parent glass, glass-ceramic and cobalt-chromium alloy are summarized in Table I.

The composites are prepared from thoroughly mixed combinations of powdered glass and suitable volume fractions of various cobalt–chromium particles. They are vacuum-hot-pressed into discs of about 38 mm diameter and 5 mm thickness. A flash-pressing technique is used, i.e. the densification pressure (30 MPa) is applied while temperature is

---

* Present address: Montpellier Chirurgie, "Le Nobel", Z. A. du Millénaire, 34000 Montpellier, France.

0022–2461

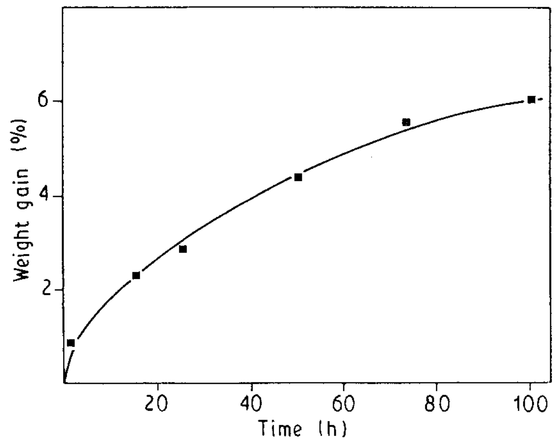

Figure 1 Weight gain of cobalt–chromium particles as a function of oxidation time.

increased up to total sintering [2, 6]. Pressure is removed as soon as samples are totally dense. They are then kept at 700 °C for 1 h to obtain ceramization of the matrix.

Most composites are obtained from seven mixtures of glass with increasing volume fractions (from 3.5–50%) of the non-oxidized smallest particles. For comparison other types of materials are also prepared; some of them with inclusions of higher diameter. Furthermore, previous works had shown that oxidation of inclusions could improve bonding between matrix and particles, which modified properties of resulting composites [7, 9]. Therefore some composites are made with the same volume fraction (30%) of the differently oxidized particles. For each composition two or three discs are prepared.

2.2. Methods of measurements

2.2.1. Thermal properties

Linear thermal expansion is measured with a differential dilatometer (D.I. 10–2, Adamel–Lhomargy) using vitreous silica as a reference material. Measurements are made from room temperature to 750 °C, at a linear heating rate of 3 °C min^{-1}.

The relative expansion at each temperature, and the average linear thermal expansion coefficients are deduced from the recorded curves [2].

2.2.2. Elastic properties

Elastic properties are measured by a dynamic method based on the magnetostrictive effect [2, 10].

Only Young's modulus can be obtained using square shaped bars as specimen resonators. Discs must be used for the determination of both Young's modulus and Poisson's ratio.

The knowledge of two elastic constants allows us to calculate the others [2, 11, 12].

2.2.3. Mechanical properties

Flexural strength, σ_R, and fracture toughness, K_{IC}, are measured on square shaped bars, which are cut directly from hot-pressed discs or from samples used previously for elastic properties measurements.

Three point bend fracture strength determinations are conducted on $1.5 \times 3 \times 15\ \text{mm}^3$ bars; the outer knife edge spacing is 12 mm. The Instron testing machine operates at a loading rate of 0.1 mm min^{-1}. All measurements are made in air at room temperature. For each composite, seven to sixteen specimens are fractured.

Toughness values are determined using $2 \times 4 \times 24\ \text{mm}^3$, SENB specimens, which are fractured in three point bending over a 16 mm span. A notch as thin as possible of about 1.3 mm depth is machined at the midpoint of one 24 mm edge of each specimen. Samples (two to nine for each composite) are tested at a cross-head speed of 0.05 mm min^{-1}. All measurements are carried out in air at room temperature.

Fracture toughness is calculated from specimen dimensions, notch depth and critical load for fracture [2, 13]. As was shown previously, such conditions allow us to reach true initiation K_{IC} factor [13–16]. The knowledge of K_{IC} and σ_R allows us to calculate other mechanical characteristics: critical flaw size, a_c, initiation fracture energy, Γ.

Critical flaw size (the size of the defect responsible for the failure) may be obtained from [17, 18]

$$a_c = \left[\frac{Z K_{IC}}{Y \sigma_R}\right]^2 \qquad (1)$$

where Y is a dimensionless term that depends on the crack depth and the test geometry [13], and Z is

TABLE I Properties of materials for the preparation of glass–ceramic CAP–cobalt–chromium composites

Properties		Glass CAP	Glass–ceramic CAP	Cobalt–chromium 788 alloy
Density (g cm^{-3})		2.64	2.65	8.3
Average linear expansion coefficients ($10^6 \times$ °C^{-1})	α_{20-500}	9.3	16.7	12^a
	α_{20-700}	–	16.4	13^a
Young's modulus (GPa)		64	68	230
Poisson's ratio		0.256	0.180	0.27
Fracture stress (MPa)		53.9	146.7	700 $\sigma_Y = 500$
Fracture toughness (MPa $\times$ m$^{1/2}$)		0.78	2.22	–
Average radius of particles (μm)		50	–	11

^{a} values given by the manufacturer

another dimensionless quantity that depends on the configuration of the crack [17].

In the case of plane strain, Γ is given by [19]

$$\Gamma = \frac{K_{IC}^2}{2E}(1 - \nu^2) \quad (2)$$

where E is Young's modulus, and ν is Poisson's ratio.

To use this equation, it is necessary to ensure that a condition of plane strain is really obtained and also that the strain cannot be relieved by general plastic deformation. These conditions are fulfilled provided that the depth, a, of the notch and the width, b, of the samples are higher or equal to $(K_{IC}/\sigma_Y)^2$, where, σ_Y, is the yield stress [14, 20].

It was shown previously that these equations are nearly always satisfied for such composites [21].

3. Results and discussion

Most results and discussions focus on composites made with the smallest non-oxidized particles. The behaviour of the other composites will be explained only for comparison.

3.1. Thermal properties

3.1.1. *Thermal properties of cobalt–chromium alloy*

The linear expansion of the pure alloy has been studied and the average coefficients have been calculated between 20 and 500 °C, 20 and 700 °C, respectively. These experimental values α_{exp} have then been compared with those α_{man} given by the manufacturer; in both temperature ranges, a significant difference has been noticed between both values, since they are, respectively;

$$\alpha_{man(20-500)} = 12 \times 10^{-6}\,°C^{-1}$$

$$\alpha_{exp(20-500)} = 14.4 \times 10^{-6}\,°C^{-1}$$

$$\alpha_{man(20-700)} = 13 \times 10^{-6}\,°C^{-1}$$

$$\alpha_{exp(20-700)} = 15.2 \times 10^{-6}\,°C^{-1}$$

These high discrepancies lead us to wonder whether the experimental values, measured on a dense cylinder of 788 alloy, are the true coefficients of the metallic powder. The thermal study of composites permits us to have a more precise idea on this problem.

3.1.2. *Thermal properties of composites*

The expansion curves of cobalt–chromium composites (Fig. 2) shows a shoulder between 100 and 200 °C which is due to $\alpha \rightleftarrows \beta$ transformation of $AlPO_4$ cristobalite form [22–24] in the glass–ceramic matrix. Sometimes, other features also occur at higher temperatures. Those which are observed close to 500 °C could be due to the residual vitreous phase of the matrix (Fig. 2 – dotted line).

The average linear thermal expansion coefficients have also been calculated between 20 and 500 °C (α_{20-500}), 20 and 700 °C (α_{20-700}), respectively. The coefficients α_{20-500} slightly decrease as a function of cobalt–chromium volume fraction, c_p (Fig. 3a and b). For the coefficients α_{20-700}, the decrease is not so clear (Fig. 3c and d); some values seemed to be disturbed by the features at high temperature. The oxidation of particles has no significant influence on the value of thermal expansion coefficients (Table II).

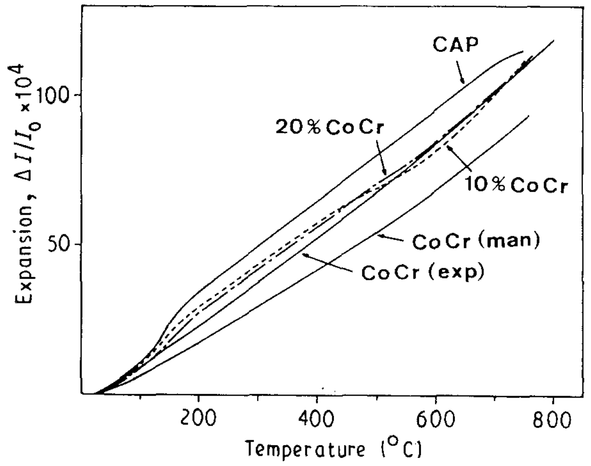

Figure 2 Linear thermal expansion of glass–ceramic CAP–cobalt–chromium composites.

These experimental data have been compared with various models, which predict theoretical evolutions of α as a function of c_p and in terms of the thermal and elastic properties of the components [25–27] (Fig. 3). In each temperature range (20–500 °C or 20–700 °C), when α_{788} is taken equal to α_{exp} ($14.4 \times 10^{-6}\,°C^{-1}$ or $15.2 \times 10^{-6}\,°C^{-1}$) in calculations, most experimental values fall below the lowest curve (Turner's model [25] – Fig. 3a and c). This probably means that: 1. both values α_{exp} are overestimated; 2. they are not the true coefficients of 788 powdered alloy as suggested above. In fact, when calculations are made with α_{man} ($12 \times 10^{-6}\,°C^{-1}$ and $13 \times 10^{-6}\,°C^{-1}$), most experimental average expansion coefficients lie within theoretical curves (Fig. 3b and d). However, these values α_{man} could underestimate the coefficients of 788 alloy, since it can be shown that most experimental values fit well with Turner's curves (Fig. 3a and c – dashed lines) calculated, respectively, with

$$\alpha_{788(20-500)} = 13.7 \times 10^{-6}\,°C^{-1}$$

$$\alpha_{788(20-700)} = 14.2 \times 10^{-6}\,°C^{-1}$$

Because of this, these values will be further considered as the true coefficients of 788 powdered alloy.

3.2. Elastic properties

Young's modulus increases with the volume fraction, c_p, of cobalt–chromium alloy (Table III). No effect on particles size is noticed (Table IV). The oxidation of

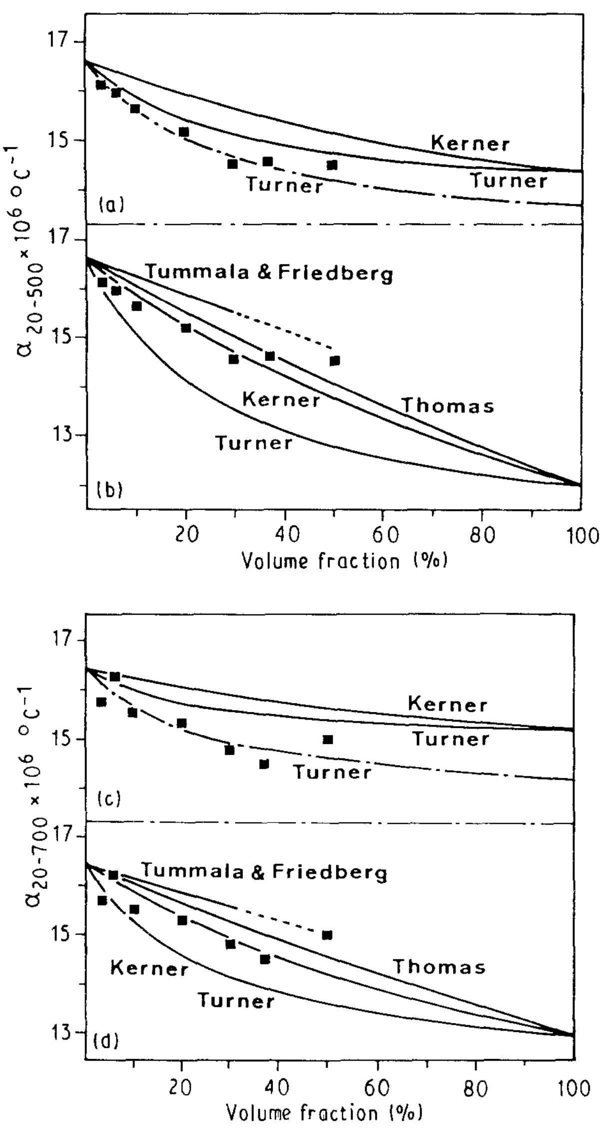

Figure 3 Theoretical and experimental average linear thermal expansion coefficients of glass–ceramic CAP–cobalt–chromium composites: (a) and (b) α_{20-500}; (c) and (d) α_{20-700}.

particles does not produce significant changes of elastic properties.

The experimental results have been compared with values given by various models. These expressions predict theoretical evolution of Young's modulus of composites as a function of volume fraction of the second phase and from the elastic properties of individual components [27, 30–33]. Most of them have representative curves lying within two limits: the upper bound, Voigt model [31] and the lower bound, Reuss model [32]. These models assume that strains and stresses are totally transferred from one phase to the other, which requires both a close contact between matrix and particles and no microcracking of materials.

TABLE II Thermal properties of composites glass–ceramic CAP–cobalt–chromium oxidized particles (30% volume)

Oxidation times (h)	Average linear thermal expansion coefficient ($\times 10^6\ ^\circ C^{-1}$) α_{20-500}	α_{20-700}
0	14.6	14.8
1	14.7	15.5
15	14.0	14.3
100	14.5	14.5

Fig. 4 shows that all experimental values fall within Hashin and Shtrickman's upper (u.b.) and lower (l.b.) bound [33], which means that both conditions noticed above are fulfilled in glass–ceramic–cobalt–chromium systems.

In these composites, the coefficient of thermal expansion of the matrix is slightly greater than that of cobalt–chromium alloy. A residual stress field is developed within and around particles as the body cools from ceramization temperature (700 °C). Since cobalt–chromium particles are spherical each of them is subjected to a uniform hydrostatic pressure, which may be calculated using Selsing's equation [34]:

$$P_0 = \frac{\Delta\alpha\Delta T}{\dfrac{1+\nu_m}{2E_m} + \dfrac{1-2\nu_p}{E_p}} \tag{3}$$

where $\Delta\alpha = \alpha_m - \alpha_p$; ΔT is the difference between ceramization and room temperature (680 °C); ν_m and ν_p are the Poisson's ratio of matrix and particles, respectively; E_m and E_p are the Young's modulus of matrix and particles, respectively.

Substituting reported values in Equation 3 then

$$P_0 = 140\ \text{MPa}$$

The tangential stress outside particles is [19, 35]

$$\sigma_{\theta\theta} = \frac{P_0}{2}\left[\frac{R}{r}\right]^3 \tag{4}$$

TABLE III Elastic and mechanical properties of glass–ceramic CAP–cobalt–chromium composites

Cobalt–chromium fraction (vol %)	Young's modulus (GPa)	Poisson's ratio	Fracture stress (MPa)	Fracture toughness (MPa $\times$ m$^{1/2}$)	Critical flaw size (μm) Griffith flaw[a]	penny-shaped crack[b]
0	68	0.180	146.7	2.22	60	145
3.5	70	0.191	144.2	2.17	60	145
6	71.5	0.193	140.6	2.16	62	150
10	77.5	0.198	144.3	2.16	59	143
20	87.5	0.204	139.0	2.23	68	164
30	98	0.217	141.4	2.26	67	162
37	107	0.223	148.0	2.25	61	147
50	124.5	0.231	149.6	2.29	62	150
788	230	0.270	700	–	–	–

[a] calculated using $(Z/Y)^2 = 1/1.21\ \pi$ in Equation 1 [20, 28].
[b] calculated using $(Z/Y)^2 = 2/\pi$ in Equation 1 [28, 29].

TABLE IV Elastic properties of glass–ceramic CAP–cobalt–chromium composites as a function of particles size

Volume fraction (%) Average diameter (μm)	20		30		37		50	
	E (GPa)	ν	E (GPa)	ν	E (GPa)	ν	E (GPa)	ν
22	87.5	0.204	98	0.215	107	0.223	124.5	0.233
40	86	0.207	96	0.214	105	0.223	125	0.233
60	–	–	–	–	104	0.220	113	0.226

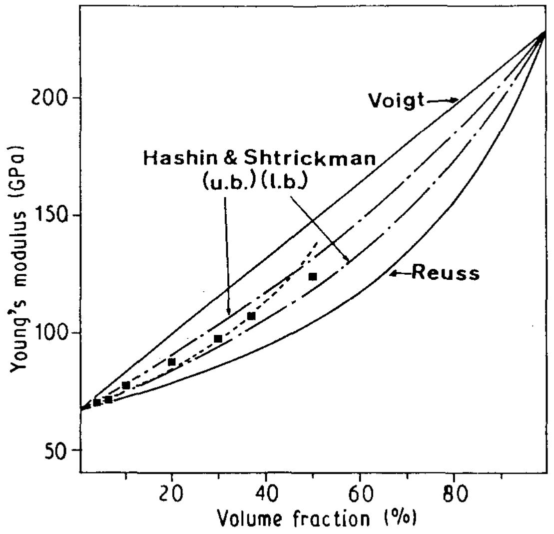

Figure 4 Theoretical and experimental Young's modulus of glass–ceramic CAP–cobalt–chromium composites.

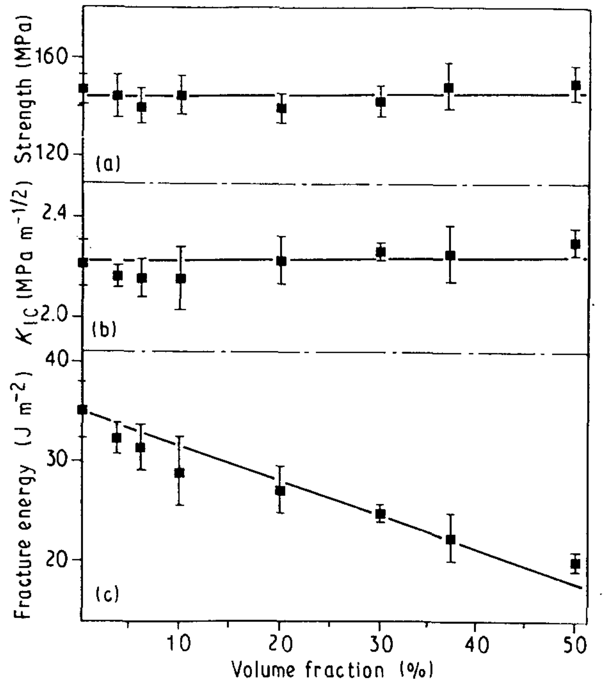

Figure 5 Mechanical properties of glass–ceramic CAP–cobalt–chromium composites: (a) fracture stress; (b) fracture toughness and (c) fracture energy (linear approximation).

where R is the radius of the particle, and r is the distance from the centre of the particle.

The maximum reached for $r = R$, is only 70 MPa, which is probably too low to initiate radial cracks originating from the particle–matrix interface, as was observed previously in systems with high thermal mismatch [19, 35–38]. In fact, Krstic analysis [35] shows that particles should have a radius of at least 200 μm to allow crack initiation. Since the average radius of cobalt–chromium particles is equal to 11 μm the occurrence of a microcracking is totally unrealistic. Moreover even though particles are not (or poorly) bonded to the matrix, pressure, P_0, ensures at least a mechanical contact between both phases. These materials thus, have a good integrity, which explains the agreement between experimental values and theoretical models. The effect of P_0 also explains why a possible improvement of bonding by oxidation of particles does not modify the elastic properties significantly.

3.3. Mechanical properties

Mechanical properties (Table III) have been studied as a function of cobalt–chromium volume fraction, c_p; in each diagram, the upper and lower bound of each average value is calculated by a Student t-test at 5% significance level.

In a first approximation, σ_R does not show significant evolution; it remains close to σ_{Rm} (Fig. 5a). In the range of metal volume fractions studied, this system can therefore be considered as a constant stress to failure system

$$\sigma_R = \sigma_{Rm} \quad (5)$$

Fracture toughness can also be considered approximately as a constant from 0–50% inclusions (Fig. 5b)

$$K_{IC} = K_{ICm} \quad (6)$$

Neglecting the influence of Poisson's ratio ($1 - \nu^2 = 1 - \nu_m^2$), then

$$\Gamma E = \Gamma_m E_m \quad (7)$$

where Γ_m is the fracture energy of the matrix.

Fracture energy continuously decreases from 0–50% inclusions. This decrease (Fig. 5c) agrees, in a first approximation, with

$$\Gamma = \Gamma_m(1 - c_p) \quad (8)$$

This expression based on typical stereology [12] means a planar surface fracture; scanning electron micrograph of this surface (Fig. 6a) does not show very significant surface irregularities. The expression also means that cobalt–chromium particles are not bonded to the matrix c_p is thus a pseudo-pore volume fraction [39]. This is also shown by scanning electron microscopy (Fig. 6b): the fracture propagates towards cobalt–chromium spheres and around them at the interface. Hemispherical cavities remain as evidence of

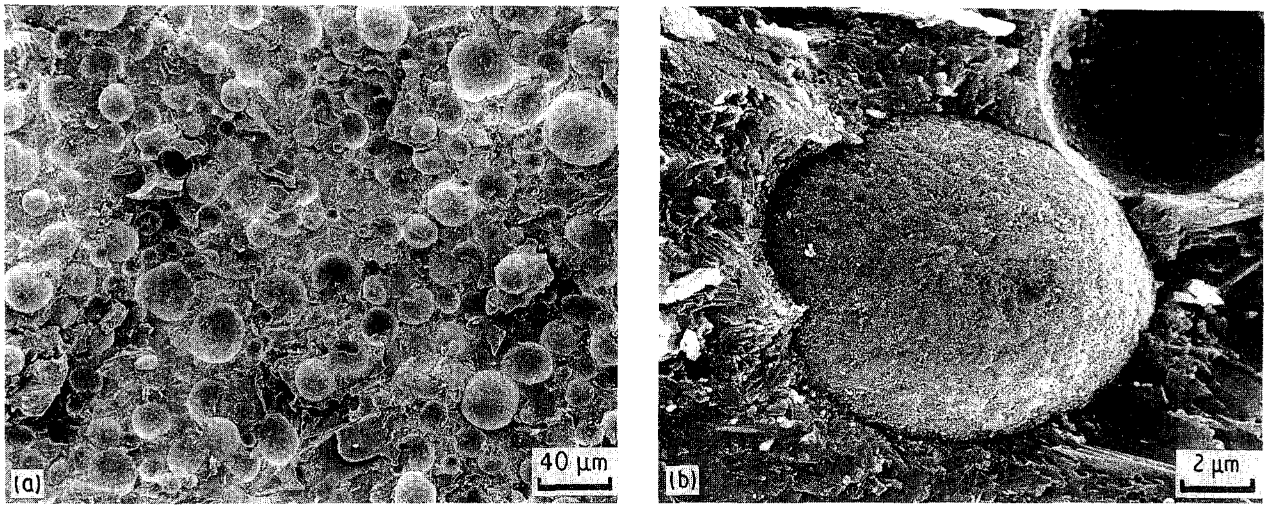

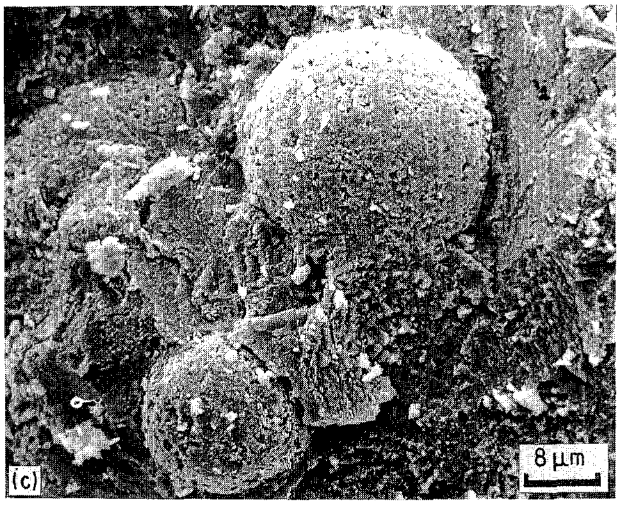

Figure 6 Fracture surface in glass–ceramic CAP–cobalt–chromium composites: (a) general view of the surface with non-oxidized particles; (b) detailed view of the same surface and (c) detailed view with oxidized particles.

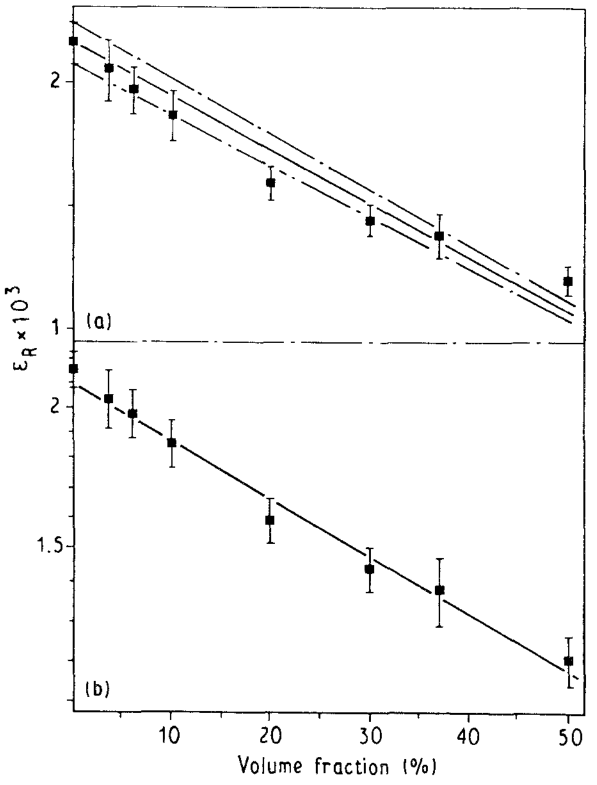

Figure 7 Strain in glass–ceramic CAP–cobalt–chromium composites: (a) linear approximation and (b) exponential law.

spheres in the opposite fracture surface. This behaviour was expected because it relieved the biaxial tension resulting from the internal stress.

Dividing Equation 8 by Equation 7, then

$$\frac{1}{E} = \frac{1 - c_p}{E_m} \tag{9}$$

Besides Hashin and Shtrickman's relations [32], the evolution of Young's modulus as a function of c_p can also be expressed, in a first approximation, by a Reuss's law [31] (Fig. 4 – dotted line), where the term, c_p/E_p, would be negligible, which means that E_p would tend to infinity. This last conclusion can also be expressed differently: dividing Equation 5 by Equation 9 member to member

$$\frac{\sigma_R}{E} = \frac{\sigma_{Rm}}{E_m}(1 - c_p) \tag{10}$$

Since cobalt–chromium composites show a brittle fracture, Equation 10 becomes, from Hooke's law

$$\varepsilon_R = \varepsilon_{Rm}(1 - c_p) \tag{11}$$

In a first approximation, the evolution of strain, ε_R, as a function of c_p is linear (Fig. 7a – continuous line). Two other straight lines are also drawn (Fig. 7a – dashed lines) using, in Equation 11, the values ε_{Rm^+} and ε_{Rm^-}, which are calculated from the upper σ_{Rm^+} and lower σ_{Rm^-} bound of σ_{Rm}. Equation 11 also means that cobalt–chromium composites behave as if only matrix strained during fracture tests.

In practice, this is not totally true: Young's modulus of cobalt–chromium 788 (230 GPa), is less than four times Young's modulus of glass–ceramic CAP (68 GPa). Consequently, some experimental results do not lie within both limit straight lines Fig. 7a. A best fit of these values (Fig. 7b) is obtained by the expression

$$\varepsilon_R = \varepsilon_{Rm} e^{-bc_p} \tag{12}$$

with $b = 1.17$ and $\varepsilon_{Rm} = 2.10 \times 10^{-3}$.

Dividing Equation 12 by Equation 5 gives

$$\frac{1}{E} = \frac{1}{E_m} e^{-bc_p} \qquad (13)$$

This is another expression $E = f(c_p)$, besides Equation 9 and Hashin and Shtrickman's model [32].

Combining Equation 13 with Equation 7 leads to

$$\Gamma = \Gamma_m e^{-bc_p} \qquad (14)$$

Using for Γ_m both values Γ_{m^-} and Γ_{m^+} defined as σ_{Rm^-} and σ_{Rm^+} previously, two limit curves can be drawn (Fig. 8). For all cobalt–chromium composites, experimental fracture energies lie within both these curves.

Such a relation, which has already been proposed for porous materials [12, 40], is thus still valid for *pseudo*-porous systems even if matrix contracts around cobalt–chromium microspheres on cooling from fabrication temperature.

This relation means that crack seeks the path having the minimum solid area, i.e. the maximum, not the average cross-sectional area of porosity as given by stereology [12].

As was explained previously, all these results deal with cobalt–chromium composites made with the non-oxidized smallest particles. For the same volume fraction, when particle diameter is increased, strength decreases significantly (Fig. 9a), as already seen in other pseudo-porous systems [41]. The other mechanical properties also decrease (Fig. 9b and c).

When particles are oxidized, the glass is saturated, during hot-pressing, with the oxide of the metal, at the glass–metal interface; a bond between matrix and particles is thus obtained [8, 41]. As a result, mechanical properties increased continuously with the oxidation rate defined as the weight gain percentage (Fig. 10). For fracture toughness and fracture energy, this increase is linear (Fig. 10b and c). The more particles oxidized, the stronger the bond. Glass–ceramic adhering to cobalt–chromium microspheres can be seen on a scanning electron micrograph of the fracture surface (Fig. 6c). It also shows that, in spite of the bond, fracture proceeds directly towards cobalt–chromium microspheres and around them, close to the interface as was already seen with non-bonded particles (Fig. 6b). Crack follows this path in

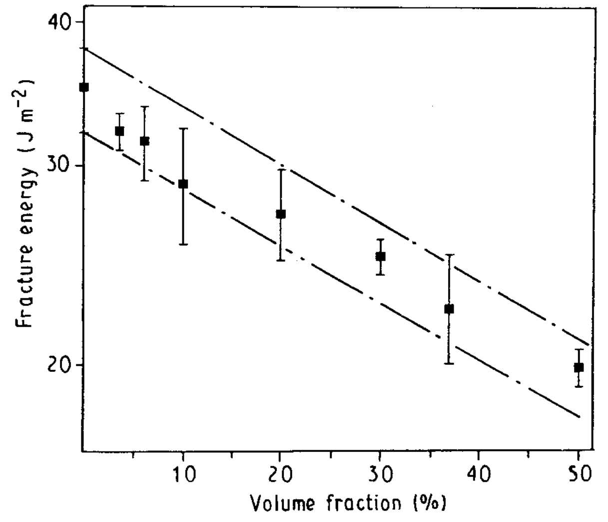

Figure 8 Fracture energy of glass–ceramic CAP–cobalt–chromium composites (exponential law).

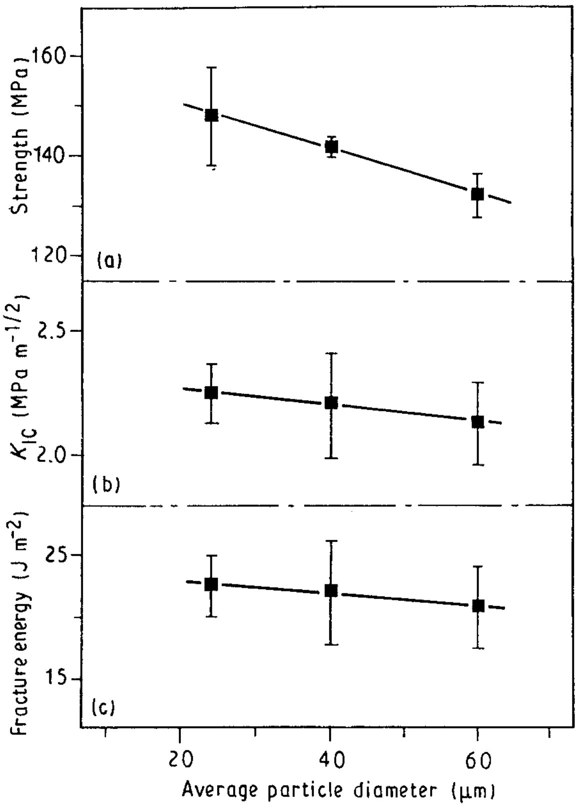

Figure 9 Mechanical properties of glass–ceramic CAP–cobalt–chromium composites as a function of particles size (composites with 37 vol % inclusions).

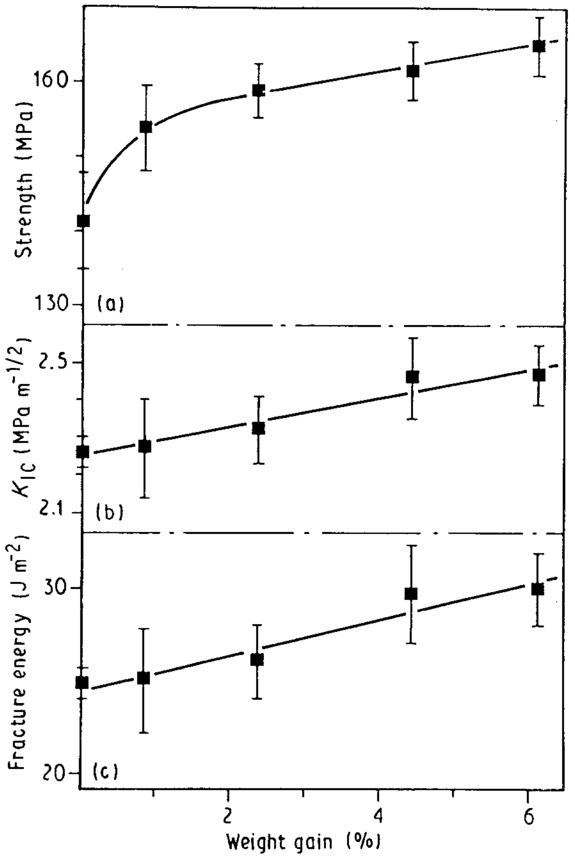

Figure 10 Mechanical properties of glass–ceramic CAP–cobalt–chromium composites as a function of weight gain of particles.

order to attempt to relieve the tangential tensile stress due to thermal mismatch [8, 19, 42]. This mismatch thus appears as being preponderant with respect to elastic mismatch. If thermal mismatch was absent, fracture would pass through the matrix as a result of elastic stress concentration at the particle pole [9, 19].

4. Conclusion

Glass–ceramic–cobalt–chromium composites could be obtained from mixtures of a calcium alumino–phosphate parent glass and various volume fractions (up to 50%) of cobalt–chromium particles. They have been prepared by hot-pressing using a flash-pressing technique.

Their elastic moduli measured by dynamic methods have been found to be in agreement with values given by Hashin and Shtrickman's theoretical expressions, which have indicated a good integrity of these composites. Since the thermal expansion of matrix is slightly greater than that of particles, the mismatch ensures a close contact between both phases; however, it is too small to induce radial crack initiation originating from the particle–matrix interface.

The contact between matrix and particles is purely mechanical, since the study of strength, toughness and particularly fracture energy shows that particles are not bonded to the matrix. This is seen by scanning electron microscopy. In this pseudo-porous system, the evolution of fracture energy, as a function of particle volume fraction, is expressed by the same exponential law as in true porous systems. This means that the crack seeks the path having the minimum solid area.

When particle size is increased, mechanical properties decreased while thermal and elastic properties are not modified significantly. Oxidation of inclusions permits the creation of a bond between matrix and cobalt–chromium microspheres, which increase both strength, toughness and fracture energy. However, since thermal mismatch already produces a contact between both phases, oxidation has no effect either on thermal or elastic properties.

References

1. J. J. MECHOLSKY, *Amer Ceram. Soc. Bull.* **65** (1986) 315.
2. R. ROGIER and F. PERNOT, *J. Mater. Sci.: Mater. Med.* **2** (1991) 153.
3. F. PERNOT, J. ZARZYCKI, F. BONNEL, P. RABISCHONG and P. BALDET, *J. Mater. Sci.* **14** (1979) 1694.
4. F. PERNOT and R. ROGIER, in "Bioceramics", Vol. 2, edited by G. Heimke (German Ceramic Society, Cologne, 1990) p. 311.
5. R. ROGIER and F. PERNOT, *J. Mater. Sci.* **26** (1991) 5664.
6. M. DECOTTIGNIES, J. PHALIPPOU and J. ZARZYCKI, *ibid.* **13** (1978) 2605.
7. M. A. STETT and R. M. FULRATH, *J. Amer. Ceram. Soc.* **51** (1968) 599.
8. *Idem, ibid.* **53** (1970) 5.
9. A. K. KHAUND and P. NICHOLSON, *J. Mater. Sci.* **15** (1980) 177.
10. J. F. W. BELL and J. M. PELMORE, *J. Phys. E: Sc. Just.* **10** (1977) 1145.
11. D. E. GRENOBLE, J. L. KATZ, K. L. DUNN, R. S. GILMORE and K. LINGA MURTY, *J. Biomed. Mater. Res.* **6** (1972) 221.
12. R. W. RICE, in Treatise on Materials Science and Technology, Vol. 11, edited by R. K. MacCrone (Academic Press, New York, 1977) p. 199.
13. W. F. BROWN and J. E. SRAWLEY, in ASTM Special Technical Publication no. 410, Baltimore, 1967, p. 1.
14. J. L. CHERMANT, F. OSTERSTOCK and G. VADAM, *Verres Réfract.* **33** (1979) 843.
15. R. W. DAVIDGE and G. TAPPIN, *J. Mater. Sci.* **3** (1968) 165.
16. A. G. EVANS, in "Fracture Mechanics of Ceramics", Vol. 1, edited by R. C. Bradt, D. P. H. Hasselman and F. F. Lange (Plenum Press, New York, 1974) p. 17.
17. A. G. EVANS and G. TAPPIN, *Proc. Br. Ceram. Soc.* **23** (1972) 275.
18. J. PHALIPPOU, T. WOIGNIER and R. ROGIER, *J. Phys.* **24** (1989) C4.
19. N. MIYATA and H. JINNO, *J. Mater. Sci.* **16** (1981) 2205.
20. J. L. CHERMANT and F. OSTERSTOCK, *ibid.* **11** (1976) 1939.
21. N. MIYATA and H. JINNO, *ibid.* **17** (1982) 547.
22. A. J. LEADBETTER and T. W. SMITH, *Phil. Mag.* **33** (1976) 105.
23. V. G. KOMLEV, I. D. KURKINA and V. A. PETROV, *Ogneupory* **12** (1979) 46.
24. W. F. HORN and F. A. HUMMEL, *J. Amer. Ceram. Soc.* **63** (1980) 338.
25. P. S. TURNER, *J. Res. Nat. Bur. Stand.* **37** (1946) 239.
26. S. J. FELTHAM, B. YATES and R. J. MARTIN, *J. Mater. Sci.* **17** (1982) 2309.
27. E. H. KERNER, *Proc. Phys. Soc.* **B 69** (1956) 808.
28. R. PABST, *Z. Werkstofftech.* **6** (1975) 17.
29. D. J. GREEN, P. S. NICHOLSON and J. D. EMBURY, *J. Mater. Sci.* **14** (1979) 1413.
30. F. F. LANGE, in "Composites Materials", Vol. 5, edited by L. J. Broutman (Academic Press, New York, 1974) p. 1.
31. W. VOIGT, "Lehrbuch der Kristallophysik" (Teubner, Berlin, 1910).
32. W. REUSS, *Z. Angew. Math. Mech.* **9** (1929) 49.
33. Z. HASHIN and S. SHTRIKMAN, *J. Mech. Phys. Sol* **11** (1963) 127.
34. J. SELSING, *J. Amer. Ceram. Soc.* **44** (1961) 419.
35. V. D. KRSTIC and M. D. VLAJIC, *Acta Metall.* **31** (1983) 139.
36. D. B. BINNS, in "Science of Ceramics", Vol. 1, edited by G. H. Stewart (Academic Press, New York, 1962) p. 315.
37. F. F. LANGE, in "Fracture mechanics of ceramics", Vol. 2, edited by R. C. Bradt, D. P. H. Hasselman and F. F. Lange (Plenum Press, New York, 1974) p. 599.
38. D. J. GREEN, *J. Amer. Ceram. Soc.* **64** (1981) 138.
39. *Idem*, PhD thesis, McMaster University, Ontario, 1977.
40. R. W. RICE, S. W. FREIMAN, R. C. POHANKA, J. J. MECHOLSKI Jr and C. C. WU, in "Fracture Mechanics of Ceramics", Vol. 4, edited by R. C. Bradt, D. P. H. Hasselman and F. F. Lange (Plenum Press, New York, 1978) p. 849.
41. J. A. PASK and R. M. FULRATH, *J. Amer. Ceram. Soc.* **45** (1962) 592.
42. R. L. BERTOLOTTI and R. M. FULRATH, *ibid.* **50** (1967) 558.

Received 15 February
and accepted 20 June 1991